

proximations to conditions that allow meandering channels in nature to develop sinuosities within the range found in simulations [see, for instance, (18) and (3)]. Howard's simulator uses a convolution integral to describe the memory effect of upstream meanders on migration rate at any given site along the river (7). It represents the river as a one-dimensional series of points along the river midline. For each iteration, the position of each point is recalculated starting at the upstream end, which is fixed. The points are moved according to the rate of laterally directed bank erosion in each point. The local rate of migration is assumed to be proportional to the curvature-dependent deviation of the thalweg path from the channel center line, measured as a near-bank velocity perturbation, $u_{c,x}$, which is described in the form of a convolution integral [see Parker and Andrews (8); D. Furbish *J. Geol.* **16**, 752 (1988)], and D. Furbish [see (4)]:

$$u_{c,x} = mC_{w,x} + n \int_A^x e^{-\beta x'} C_{w,x-x'} dx'$$

The integral describes the cumulative upstream effect of centrifugal forces and shoaling of flow over the point bar. $C_{w,x}$ is dimensionless channel center-line curvature, m , n , and β are constants, and x' is distance upstream from any given point x . A is a cutoff indicating the range of effective memory (the memory is nominally infinite, but in practice distinguishable information is not carried more than three to five bends downstream). The cutoff process is representative in the model by a simple decision rule, whereby any two non-neighbor points along the river cause the segment between them to be cut off if they are closer to each other than a set distance between one and two width units. In the simulations, I used a value of 0.3 for the input parameter k (nominal erosion rate), 0.01 for the bank resistance factor R , 0.5 for the Froude number F , and 0.2 for b (a measure of regional gradient that varies between 0 and 1).

9. A. Einstein, *Die Naturwissenschaften* **12**, 223 (1926); A. J. Odgaard, *Water Resour. Res.* **23**, 1225 (1987); M. A. Falcon Ascanio and J. F. Kennedy, *J. Fluid Mech.* **133**, 1 (1983).
10. J. M. Hooke, *Geomorphology* **14**, 235 (1995); J. Brice, *Geol. Soc. Am. Bull.* **85**, 581 (1974); S. M. Gagliano and P. C. Howard, in *River Meandering*, C. M. Elliott, Ed. (American Society of Civil Engineers, New York, 1984), pp. 147-158; G. W. Lewis and J. Lewin, *Spec. Publ. Int. Assoc. Sedimentol.* **6**, 145 (1983); J. M. Hooke and C. E. Redmond, in *Dynamics of Gravel Bed Rivers*, P. Billi et al., Eds. (Wiley, Chichester, UK, 1992), pp. 549-563.
11. K. Hasegawa, in *River Meandering*, S. Ikeda and G. Parker, Eds. (American Geophysical Union, Water Research Monograph, vol. 12, Washington, DC, 1989), pp. 215-235.
12. H. Chaté, *Nonlinearity* **7**, 185 (1994); _____ and P. Manneville, *Physica D* **32**, 409 (1988).
13. A mean sinuosity of ≈ 3.14 is independent of b , R , and F over most of the range of these parameters (8). Also, simulations with rivers of different length showed that the standard deviation is an inverse function of the length of the river, whereas the mean is length-independent. The length dependence of sinuosity variance has no bearing on the scaling relations shown in Fig. 4, B and C, as both the magnitude of the scaling range and the fractal dimension are invariant with respect to river length (the variance dependence affects only the position of the scaling interval).
14. Consider the river fractal geometry idealized in the form of a perfectly symmetrical hierarchy of bends (with increasing wavelength) that are all cuts of a circle. Represent the actual planform as an initially straight line ($s = 1$), which is then superimposed on the undulations of bends. Each hierarchical level n contributes a component $s_n - 1$ to the sinuosity of the structure. At the smallest level, $n = 1$, the bends may be represented on the average as semicircles, so that $s_1 - 1 = \pi/2 - 1 \approx 0.5715$. The total sinuosity is

$$s = 1 + \sum_{n=1}^7 (s_n - 1)$$

The average circle cuts at each level have been

- found empirically for the simulation and the Juruá River (3). The amplitude at each level is close to 1/2, 1/2, 5/12, 4/12, 3/12, 2/12, and 1/12 times the circle section length, respectively. If we use these values, sinuosity measurements at each level yield $s \approx 1 + 0.5715 + 0.5715 + 0.440 + 0.280 + 0.172 + 0.0865 + 0.020 \approx 3.1415$.
15. If it is assumed that the river deposits sediment with a constant rate, then oxbow lakes are distributed in three dimensions purely according to the meander dynamics. Clustering then requires a threshold of areal closeness and a threshold of depth closeness. A range of possible threshold values is defined by the largest values that yield no clustering and the smallest values that generate one single, large cluster of all the oxbow lakes. Within this range, all threshold values generate power-law size-frequency distributions of one to two orders of magnitude (this scale-range appears to be limited by the finite size of the simulation).
16. B. Mandelbrot and J. R. Wallis, *Water Resour. Res.* **4**, 909 (1968); J. Feder, *Fractals* (Plenum, New York, 1988). Calculate for each iteration the accumulated departure of the sinuosity from the mean. For this derived time series, the range R is the difference between the average maximum value and the average minimum value for all possible segments of a given length. This range is normalized by dividing by S , which is the standard deviation of the mean sinuosity for the whole time series. Then R/S is scaled against the segment length or lag. A power-law interval indicates temporal scaling of the original sinuosity time series. The exponent is known as the Hurst exponent and is a measure of

persistence of trends. A Hurst exponent of $H = 0.54$ reflects the appearance of "white noise" generated by chaos due to weak information-storage capacity and is observed as an absence of long-range correlations in time or space.

17. The fractal dimension, D , for the river planform as a whole is given by $N = ar^{-D}$, where r is the length of a yardstick in units of average river width and N is the number of yardsticks necessary to cover the river; a is a proportionality constant.
18. V. R. Baker, in *Fluvial Sedimentology*, A. D. Miall, Ed. (Canadian Society of Petroleum Geologists, Memoir vol. 5, Calgary, 1978), pp. 211-230.
19. Heraclitus, *On Nature* [fragments translated by P. Wheelwright, *Heraclitus* (Princeton Univ. Press, Princeton, NJ, 1959)]; G. S. Kirk, *Heraclitus, The Cosmic Fragments* (Cambridge Univ. Press, Cambridge, 1952); F. Nietzsche, *The Will to Power* [Random House (Vintage Books), New York, 1967]; G. Deleuze, *Nietzsche and Philosophy* (Athlone Press, London, 1983), pp. 47-49.
20. I thank A. Howard for generously making his simulator available for this study. I am grateful to P. Español for contributions to an earlier version of this report and for discussions. P. Bak, P. F. Friend, K. Richards, G. Stephens, and P. Charity suggested many improvements. L. Rush wrote the analysis programs. This research was supported by British Gas plc, Oryx (UK) Energy plc, Department of Trade and Industry (DTI), the Norwegian Research Council (NFR), and the British Council.

13 September 1995; accepted 3 January 1996

High-Temperature Study of Octahedral Cation Exchange in Olivine by Neutron Powder Diffraction

C. M. B. Henderson,* K. S. Knight, S. A. T. Redfern, B. J. Wood

Time-of-flight, neutron powder diffraction to 1000°C provides precise octahedral site occupancies and intersite distribution coefficients for MnMgSiO₄ and MnFeSiO₄ olivines. Intersite exchange occurs in minutes down to 500°C. Equilibrium distribution coefficients show that manganese ordering into the larger octahedral site decreases with increasing temperature. Exchange energies are 15.7 and 10.1 kilojoules per mole for magnesium-manganese and iron-manganese, respectively. Distribution coefficients deduced for FeMgSiO₄ olivine suggest an exchange energy of 4.8 kilojoules per mole. Intersite exchange energies are consistent with diffusion coefficients in the order iron > magnesium > manganese. Geothermometry based on magnesium-manganese and iron-manganese exchange may be possible only for samples equilibrated below 500°C.

As olivine [(Mg,Fe,Mn)₂SiO₄] is the major constituent of the Earth's upper mantle, its physical properties dominate the deep Earth's geophysical and geochemical properties down to the 410-km seismic discontinuity, which is attributed to the transitions of olivine to β - and γ -spinel-type polymorphs. A common simplifying assumption is that olivine is near ideal, with Mg and Fe fully disordered over M1

and M2, the two octahedral sites. Intracrystalline M-site partitioning would, however, be expected to modify olivine's thermodynamic stability, the diffusion rates of M-site metals, and (potentially) its elastic parameters. Furthermore, if significant partitioning does occur, M-site occupancies might also provide a means of using olivine as a petrogenetic indicator for thermometry and speedometry in a wide range of rocks.

Crystal chemical studies of olivines, primarily at room temperature (T) and pressure (P), show that divalent cations tend to order preferentially between M2, the larger site, and M1, the more distorted site; for example, Fe, Ni, and Zn into M1, and Mn and Ca into M2 (1). Early at-

C. M. B. Henderson, Department of Earth Sciences, University of Manchester, Manchester M13 9PL, UK.
K. S. Knight, ISIS, Rutherford Appleton Laboratory, Oxon OX11 0QX, UK.
S. A. T. Redfern, Department of Earth Sciences, University of Cambridge, Cambridge CB2 3EQ, UK.
B. J. Wood, Department of Geology, University of Bristol, Bristol BS8 1RJ, UK.

*To whom correspondence should be addressed.

tempts to determine the T dependence of partitioning involved study at room T and P of samples quenched from high T , mainly in the Mg-Fe (2) and Mg-Mn (3) olivine systems; contradictory data were obtained, likely because M1-M2 reequilibration occurred during quenching. It has been shown that Mg-Fe intersite equilibration at 1000°C occurs in about 1 s, that reordering upon cooling occurs on a time scale of about 10 ms, and that blocking T s appear to be between 500° and 800°C, depending on the cooling rate (4). Rapid exchange has recently been confirmed in a theoretical study of ordering kinetics (5). The typical experimental quenching rates are too slow to freeze-in the equilibrium high- T ordering states. In situ experiments are, therefore, essential for studying ordering in such mineral systems. No significant changes in Fe-Mg ordering were detected up to 800°C by in situ powder x-ray diffraction (XRD) (6). By contrast, high- T XRD, single crystal studies (7) suggest that Fe is slightly ordered into M1 [$K_D^{\text{Fe-Mg}} = 1.1$ to 1.2 (8)], and that with increasing T this ordering increases [for example, $K_D^{\text{Fe-Mg}} = 1.37$ at 900°C (9)]. However, recent high- T neutron diffraction, single crystal work (10) shows that $K_D^{\text{Fe-Mn}}$ increases from 1.02 at room T to about 1.46 at 800°C, followed by a progressive decrease, falling to 0.19 at 1300°C. This trend indicates that Fe orders into M1 up to about 950°C, but this behavior is reversed at higher T s with substantial partitioning into M2.

More precise structural information for olivines at high T s is necessary to obtain clearer K_D versus T trends. The precision to which Fe-Mg K_D s may be determined by x-ray methods is limited both by the rapid fall-off of form factors and the inherent limits on obtaining data at short scattering vectors, whereas the precision of neutron time-of-flight diffraction measurements is constrained by the neutron scattering contrast between Fe and Mg nuclei. We have used a different approach, namely, investigating the process of cation exchange in a broader context using Mn analogs. Aspects of the fundamental characterization of cation exchange thus obtained can be used to interpret the expected behavior of Fe-Mg nonideality. To this end, time-of-flight, neutron powder diffraction data for olivine analogs were obtained at the ISIS facility, Rutherford Appleton Laboratory, using the POLARIS diffractometer (11). We have studied synthetic FeMnSiO_4 and MgMnSiO_4 olivines (12) to take advantage of the large contrast in coherent neutron scattering lengths between the pairs Fe-Mn and Mn-Mg [Fe, 9.54 fm; Mg, 5.375 fm; Mn, -3.73 fm (1 fm = 10^{-15} m)]. We were also able to obtain data over a wide range of scat-

tering vectors, allowing good discrimination of occupancies and displacement factors so that precise site occupancy factors and K_D values for Fe-Mn and Mg-Mn olivines were obtained (13) (Table 1 and Fig. 1).

By combining measured K_D values for the two samples at the same T , the T dependence for $K_D^{\text{Fe-Mg}}$ was approximated as

$$K_D^{\text{Fe-Mn}} = \frac{(\text{Fe/Mn})_{\text{M1}}}{(\text{Fe/Mn})_{\text{M2}}} \quad (1)$$

$$K_D^{\text{Mg-Mn}} = \frac{(\text{Mg/Mn})_{\text{M1}}}{(\text{Mg/Mn})_{\text{M2}}} \quad (2)$$

$$K_D^{\text{Fe-Mg}} = \frac{K_D^{\text{Fe-Mn}}}{K_D^{\text{Mg-Mn}}} = \frac{(\text{Fe/Mg})_{\text{M1}}}{(\text{Fe/Mg})_{\text{M2}}} \quad (3)$$

where $K_D = 1$ for complete disorder.

The measured $K_D^{\text{Fe-Mn}}$ value of 4.21 for the Fe-Mn olivine (Fig. 2A) at room T confirms earlier observations that Fe is ordered onto M1 and Mn onto M2 (1); this K_D represents the degree of order quenched-in during sample cooling. With increasing T , no significant change occurs until about 400°C, where K_D begins to show a small increase, reaching 5.03 at 500°C. This increase occurs because at such T s, the sample approaches the equilibrium order. With further increase to 1000°C, there is a steady, slightly nonlinear decrease in $K_D^{\text{Fe-Mn}}$ to 2.70. Upon heating, the $K_D^{\text{Fe-Mn}}$ value at 600°C is the same (4.21) as that measured at room T at the

start of the experiment, suggesting that the blocking T for Fe-Mn exchange during the rapid quench from the sample synthesis T was close to 600°C. The decreasing $K_D^{\text{Fe-Mn}}$ with increasing T corresponds to the sample becoming less ordered.

Upon stepwise cooling (at about 0.4° per second) down to 500°C, $K_D^{\text{Fe-Mn}}$ values coincide with those measured on heating. This trend defines a blocking T as low as 500°C, consistent with the slower cooling rate of our experiments allowing equilibration at lower T than occurred during quenching after synthesis. Figure 3 shows idealized paths for such ordering patterns and demonstrates the dependence of blocking T and low- T K_D value on cooling rate. Data points between 550° and 1000°C, when plotted on an Arrhenius-type diagram of $\ln K_D$ versus $1/T$, define an energy for Fe-Mn intersite exchange of 10.1 ± 0.3 kJ/mol. Data for the Mn-Mg olivine sample follow similar trends (Fig. 2B), but $K_D^{\text{Mg-Mn}}$ is larger than $K_D^{\text{Fe-Mn}}$ with a value of 7.5 at room T ; thus, Mg (in the Mg-Mn sample) is more strongly ordered onto M1 than Fe (in Fe-Mn olivine). The Mg-Mn sample becomes less ordered as T increases. The ordering path on heating is similar to that depicted in Fig. 2A, implying similar blocking T s for Mg-Mn and Fe-Mn exchange. Data between 500° and 1000°C define an exchange energy for Mn-Mg of 15.7 ± 0.9 kJ/mol. It therefore seems unlikely that geothermometry based on Fe-Mn and Mg-Mn

Table 1. Structural parameters for $(\text{Fe}_{0.5}\text{Mn}_{0.5})_2\text{SiO}_4$ at 100°C. Numbers in parentheses are errors in the last digits; x, y, z , fractional atomic coordinates; B_{iso} , isotropic temperature factors; S , fractional site occupancies. Space group, $Pm\bar{c}n$; cell parameters: $a = 6.17510(9)$ Å, $b = 4.86394(7)$ Å, and $c = 10.59147(16)$ Å; refinement parameters: $R_p = 2.9\%$, $R_{\text{wp}} = 2.0\%$, and $R_E = 1.7\%$.

Atom	x	y	z	B_{iso} (Å ²)	S
Fe1-Mn1	0.0000	0.0000	0.0000	0.51(2)	0.673(2)
Fe2-Mn2	0.25	0.9716(32)	0.2850(13)	0.51(2)	0.327(2)
Si	0.2500	0.4275(4)	0.0965(2)	0.37(2)	
O1	0.2500	0.7622(3)	0.0924(2)	0.73(2)	
O2	0.2500	0.2132(4)	0.4538(1)	0.72(2)	
O3	0.0389(2)	0.2875(2)	0.1641(1)	0.71(2)	

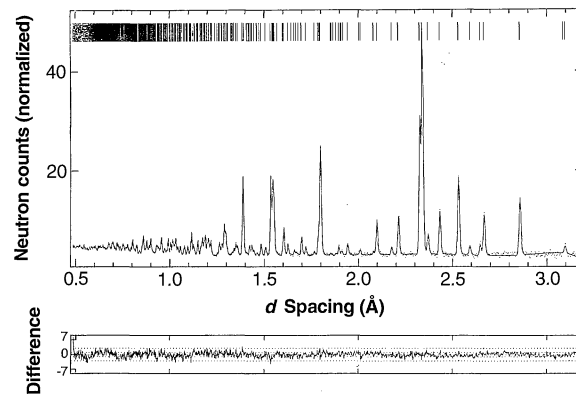


Fig. 1. Comparison of experimental (dots) and calculated (solid line) diffraction pattern for FeMnSiO_4 olivine at 100°C, together with the difference plot $[(I_{\text{obs}} - I_{\text{calc}})/\sigma_{\text{obs}}]$ (below) and theoretical peak positions (above). The dotted lines in the difference plot mark values of ± 1 and ± 3 .

exchange on M1-M2 would be possible for samples equilibrated above 500°C.

The K_D^{Fe-Mg} values for the Fe-Mg system derived from the equilibrium partitioning data for the other two samples above 500°C (Fig. 2) are <1 , suggesting that Fe is ordered onto M2 and Mg onto M1. Although this deduction contrasts with some high- T results (7, 8), it is in line with the single crystal neutron results above 900°C (10); further high- T work on Fe-Mg olivines is required to cast further light on this phenomenon. The absolute values deduced here should be treated with caution as subtle differences in the crystal chemical relations for the Fe-Mg olivine system could affect the exact order properties, but the T dependence is thought to be reliable. The deduced K_D^{Fe-Mg} values between 550° and 1000°C define an energy of Fe-Mg exchange of 4.8 ± 1.0 kJ/mol.

The low exchange energies reflect the rapid M1-M2 exchange, with the lowest energies expected to correspond to the fastest exchange rates. Thus, exchange rates should decrease in the order Fe-Mg $>$ Fe-Mn $>$ Mg-Mn. This implies that the hopping energies of intersite diffusion decrease in the order Mn $>$ Mg $>$ Fe, and hence, the relative values of the calculated volume diffusion coefficients in olivine decrease as $D_{Fe} > D_{Mg} > D_{Mn}$ (14). For the Fe-Mn sample at low T , refinement of

isothermal diffraction data collected in successive 30-min periods shows no significant structural differences, suggesting that intersite exchange equilibration occurs on a time scale of minutes (perhaps much less). Thus, K_D values determined at room T for Fe-Mn olivines (15) quenched from high T , and presumably for quenched Mg-Mn olivines (16), must be treated with caution.

The results of our in situ neutron diffraction studies on Mn analogs have wider implications for Fe-Mg natural olivines. The increasing degree of order up to about 900°C observed in high- T single crystal measurements on natural Fe-Mg olivines (7, 9, 10) might originate from the same processes as seen in our Fe-Mn data below 450°C, that is, the samples move toward equilibrium degrees of order at T s lower than the blocking T experienced during natural cooling. In addition, the fact that K_D values fall off the equilibrium K_D versus T trend at low T s (Fig. 3) offers the possibility of obtaining information on cooling rates of natural samples.

Recent structural studies of Fe-Mg order-disorder arrangements over octahedral sites in amphiboles are based on structural analyses carried out at room T on quenched samples (17), but no T dependence was detected between 600° and 750°C. Such data have been used to develop sophisticated thermodynamic mixing models (18), but before such models can be assessed, it is necessary to establish whether Fe-Mg intersite exchange is very rapid, as in olivine, or significantly slower, as in orthopyroxene (19). The contrast in Fe-Mg intersite exchange kinetics is evident when the exchange energy estimated here for olivine (4.8 kJ/mol) is compared to the value of 25 kJ/mol for orthopyroxene (20). Further high- T in situ structural work is necessary to elucidate the effects of octa-

hedral site order-disorder on structural and thermodynamic properties of mafic minerals in general.

REFERENCES AND NOTES

- G. E. Brown Jr., in *Orthosilicates*, P. H. Ribbe, Ed. (Reviews in Mineralogy, vol. 5, Mineralogical Society of America, Washington, DC, 1980), pp. 275-381.
- F. Princivalle, *Mineral. Petrol.* **43**, 121 (1990); G. Ottonello, F. Princivalle, A. Della Giusta, *Phys. Chem. Miner.* **17**, 301 (1990).
- T. Akamatsu et al., *Phys. Chem. Miner.* **16**, 105 (1988).
- N. Aikawa, M. Kumazawa, M. Tokonami, *ibid.* **12**, 1 (1985).
- T. Akamatsu and M. Kumazawa, *ibid.* **19**, 423 (1993).
- G. Artioli, M. Bellotto, B. Palosz, *Powder Diffr.* **9**, 63 (1994).
- J. R. Smyth and R. M. Hazen, *Am. Mineral.* **58**, 588 (1973); G. E. Brown and C. T. Prewitt, *ibid.*, p. 577.
- Distribution coefficients for intersite order in Fe-Mg olivines are formulated as $K_D^{Fe-Mg} = (Fe/Mg)_{M1} / (Fe/Mg)_{M2}$ (molar ratios).
- T. Motoyama and T. Matsumoto, *Mineral. J.* **14**, 338 (1989).
- G. Artioli, R. Rinaldi, C. C. Wilson, P. F. Zanazzi, *Am. Mineral.* **80**, 197 (1995); R. Rinaldi and C. C. Wilson, *Solid State Commun.* **97**, 395 (1996).
- R. I. Smith, S. Hull, A. R. Armstrong, *Mater. Sci. Forum* **166-169**, 251 (1994).
- We prepared the Fe-Mn sample by mixing Fe_2O_3 , MnO, and SiO_2 and crystallizing the mixture at 1150°C for three periods of 12 hours each, and the Mn-Mg olivine was prepared from MgO, MnO, and SiO_2 crystallized at 1400°C for three periods of 4 hours each; both were ground between heat treatments. Both samples were buffered in CO_2 -CO gas mixtures about 1 log unit more oxidizing than the Fe-FeO buffer and quenched within the reducing gas atmosphere to below 500°C in <1 min. About 3.5 g of each was prepared. Both samples were studied by x-ray powder diffraction and were found to be phase pure, with narrow peaks showing that they were well crystallized and homogeneous. Each sample was loaded into a thin-walled quartz glass tube, with silica wool separating the sample from either Fe-FeO buffer (Fe-Mn sample) or Ni-NiO buffer (Mn-Mg). The tubes were then evacuated and sealed, placed in vanadium cans, and mounted inside a vanadium furnace assembly, the whole of which was evacuated to a residual P of about 0.05 Pa. For the Fe-Mn sample, isothermal diffraction patterns were collected for 2 hours each upon heating and for 1/2 hour each upon cooling; Mg-Mn data were collected for 1 hour upon heating. Structural data were obtained by Rietveld refinement. For the Fe-Mn sample, at each T between 400° and 750°C, diffraction patterns were collected in four 1/2-hour periods. Some of these isothermal data sets were refined separately, but no differences in site populations were observed.
- Relative errors on occupancy factors for the Fe-Mn olivine are about 0.5%, equivalent to errors in K_D values of only 1 to 1.5%. Data for the Mg-Mn sample are less precise, with errors in K_D values of about 3 to 4.5%.
- M. Miyamoto and H. Takeda, *Nature* **303**, 602 (1983).
- H. Annersten, J. Adetunji, A. Filippidis, *Am. Mineral.* **69**, 1110 (1984).
- C. A. Francis and P. H. Ribbe, *ibid.* **65**, 1263 (1980).
- M. Hirschmann, B. W. Evans, H. Yang, *ibid.* **79**, 862 (1994).
- M. S. Ghiorso, B. W. Evans, M. M. Hirschmann, H. Yang, *ibid.* **80**, 502 (1995).
- J. A. Sykes-Nord and G. M. Molin, *ibid.* **78**, 921 (1993).
- G. M. Molin, S. K. Saxena, E. Brizi, *Earth Planet. Sci. Lett.* **105**, 260 (1991).
- We thank Rutherford Appleton Laboratory for research grant RB6035 and R. Rinaldi and an anonymous reviewer for constructive critical comments.

13 October 1995; accepted 1 February 1996

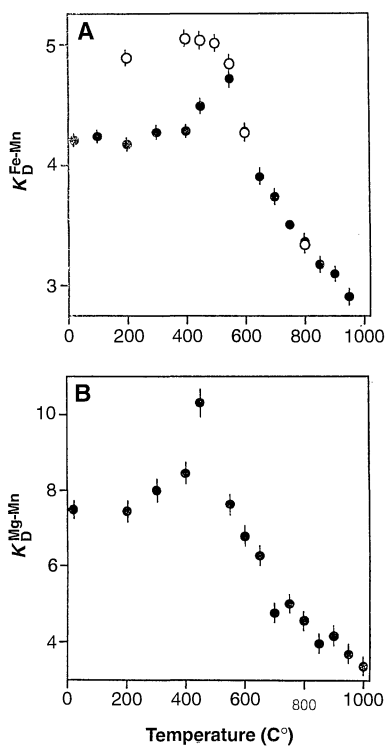


Fig. 2. Temperature dependence of the M1-M2 distribution coefficient in olivine. (A) $K_D^{Fe-Mn} = (Fe/Mn)_{M1} / (Fe/Mn)_{M2}$. (B) $K_D^{Mg-Mn} = (Mg/Mn)_{M1} / (Mg/Mn)_{M2}$. (●) Heating experiments; (○) cooling experiments. Ticks mark 1σ standard deviations.

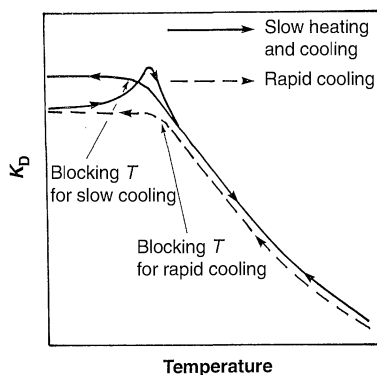


Fig. 3. Schematic variation of K_D with temperature depending on heating and cooling rates, modeled on the data for Fe-Mn olivine. The equilibrium part of the rapid cooling curve should be coincident with the slow cooling curve but is displaced for clarity.